

50. BULK PERMEABILITY OF YOUNG BACKARC BASALT IN THE LAU BASIN FROM A DOWNHOLE PACKER EXPERIMENT (HOLE 839B)¹

Terry R. Bruns² and Dawn L. Lavoie³

ABSTRACT

An inflatable drill-string packer was used at Site 839 to measure the bulk in-situ permeability within basalts cored in Hole 839B. The packer was inflated at two depths, 398.2 and 326.9 mbsf; all on-board information indicated that the packer mechanically closed off the borehole, although apparently the packer hydraulically sealed the borehole only at 398.2 mbsf. Two pulse tests were run at each depth, two constant-rate injection tests were run at the first set, and four were run at the second. Of these, only the constant-rate injection tests at the first set yielded a permeability, calculated as ranging from 1 to 5×10^{-12} m². Pulse tests and constant-rate injection tests for the second set did not yield valid data. The measured permeability is an upper limit; if the packer leaked during the experiments, the basalt would be less permeable. In comparison, permeabilities measured at other Deep Sea Drilling Project and Ocean Drilling Program sites in pillow basalts and flows similar to those measured in Hole 839B are mainly about 10^{-13} to 10^{-14} m². Thus, if our results are valid, the basalts at Site 839 are more permeable than ocean-floor basalts investigated elsewhere.

Based on other supporting evidence, we consider these results to be a valid measure of the permeability of the basalts. Temperature data and the geochemical and geotechnical properties of the drilled sediments all indicate that the site is strongly affected by fluid flow. The heat flow is very much less than expected in young oceanic basalts, probably a result of rapid fluid circulation through the crust. The geochemistry of pore fluids is similar to that of seawater, indicating seawater flow through the sediments, and sediments are uniformly underconsolidated for their burial depth, again indicating probable fluid flow. The basalts are highly vesicular. However, the vesicularity can only account for part of the average porosity measured on the neutron porosity well log; the remainder of the measured porosity is likely present as voids and fractures within and between thin-bedded basalts. Core samples, together with porosity, density, and resistivity well-log data show locations where the basalt section is thin bedded and probably has from 15% to 35% void and fracture porosity. Thus, the measured permeability seems reasonable with respect to the high measured porosity. Much of the fluid flow at Site 839 could be directed through highly porous and permeable zones within and between the basalt flows and in the sediment layer just above the basalt. Thus, the permeability measurements give an indication of where and how fluid flow may occur within the oceanic crust of the Lau Basin.

INTRODUCTION

The permeability, or the ease of fluid flow, through sediment and basalt of the oceanic crust is a key physical parameter that controls the form, magnitude, and duration of fluid flow and convection in the oceanic crust. Fluid circulation affects the amount and rate of crustal cooling and hydrothermal alteration. Permeability of oceanic basalt cannot be adequately measured from dredge or drill samples, as the permeability of the small sample does not reflect the fractures, voids, or open contacts between lava flows, which probably control permeability within the crust. A more representative estimate of the bulk permeability is obtained by measuring the permeability in situ in deep boreholes, preferably at scales large enough to include the effects of fracture and void permeability fully.

We report here the methods, data, and results of in-situ permeability measurements made during Leg 135 at Hole 839B using a drill-string packer. The measurements obtained can be combined with permeability measurements made of the overlying sediment (Lavoie et al., this volume) to gain a better understanding of the permeability and, hence, the possible fluid circulation patterns in the sediment and basalt forming the upper part of the oceanic crust in the Lau Basin.

The permeability of oceanic basalt has been measured at several sites during Deep Sea Drilling Program (DSDP) and Ocean Drilling Program (ODP) drilling, including Hole 395A (Legs 78 and 109; Becker, 1989; Hickman et al., 1984), Hole 504B (Legs 69, 83, and

111; Anderson and Zoback, 1982; Zoback and Anderson, 1983; Becker, Langseth, and Von Herzen, 1983; Becker, Langseth, Von Herzen, and Anderson, 1983; Anderson et al., 1985a, 1985b; Becker, 1989), and Hole 735B (Leg 118; Goldberg et al., 1991; Becker, 1991). In all of these sites, permeability values for the pillow basalts and flows similar to those measured at Site 839B ranged from 10^{-12} to 10^{-14} m², but mainly about 10^{-14} m². The underlying sheeted dikes and gabbros had permeability measurements as low as 10^{-18} m². An objective for measuring the permeability at Hole 839B was to compare the permeability of the young backarc crust (2 m.y. old) with the permeabilities of the older crusts sampled elsewhere.

We note here that the preliminary permeability of 2 to 8×10^{-16} m² calculated for Hole 839B and reported in the *Initial Reports* volume for Leg 135 (Parson, Hawkins, Allan, et al., 1992, pp. 460–462) is incorrect. The corrected permeability reported here for Hole 839B is 1 to 5×10^{-12} m².

SITE LOCATION AND LITHOLOGIC SUMMARY

Site 839 is located in the central Lau Basin about 225 km east of the axis of the Lau Ridge and approximately 55 km west of the active Eastern Lau Spreading Center (ELSC; Fig. 1). The site is in 2617 m of water on the edge of an elongated, northeast-trending basin (Fig. 2). Site 839 lies on the uplifted west side of the basin, flanked by a north- to northeast-trending ridge (Fig. 3; see Parson, Hawkins, Allan, et al., 1992, pp. 401–402; also Bruns et al., this volume). The uplifted and perched location of the site on the flank of the ridge could mean that the basement rocks might be more broken by faults and fractures than similar rocks beneath the basin to the east.

The seismic line across the site (Fig. 3) shows an irregular, probably faulted, basement surface and a 200- to 300-m-high, northeast-trending fault bounding the east side of the upraised sediment pond

¹ Hawkins, J., Parson, L., Allan, J., et al., 1994. *Proc. ODP, Sci. Results*, 135: College Station, TX (Ocean Drilling Program).

² Branch of Pacific Marine Geology, U.S. Geological Survey, M.S. 999, 345 Middlefield Road, Menlo Park, CA 94025, U.S.A.

³ Naval Research Laboratory—Detachment, Ocean Science Directorate, Seafloor Geosciences Division, Stennis Space Center, MS 39529-5004, U.S.A.

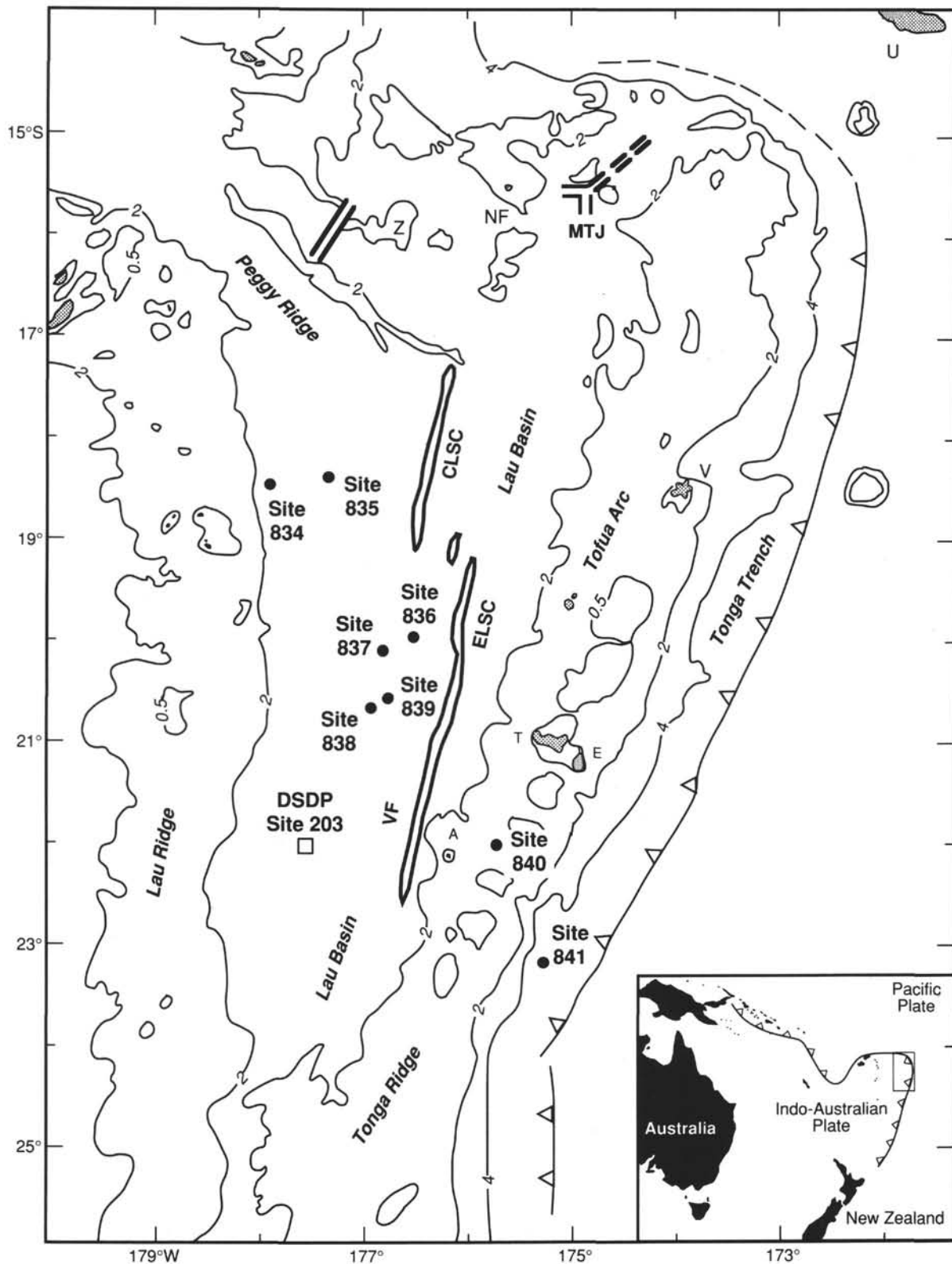


Figure 1. Bathymetric chart of the Lau Basin area and location of Site 839 and other sites drilled during Leg 135. The figure also shows the regional setting and the major geologic features of the Tonga Trench and Lau Basin system. Islands shown are Tongatapu (T), 'Eua (E), Vava'u (V), Niuafu'ou (NF), 'Ata (A), and Upolu (U). Locations of the Central Lau (CLSC) and Eastern Lau (ELSC) spreading centers, Valu Fa (VF) Ridge, Mangatolu Triple Junction (MTJ), and Zephyr Shoal (Z) are after Parson, Hawkins, Allan, et al. (1992) and references contained therein. The location of DSDP Site 203 is shown as an open square. Contours in kilometers.

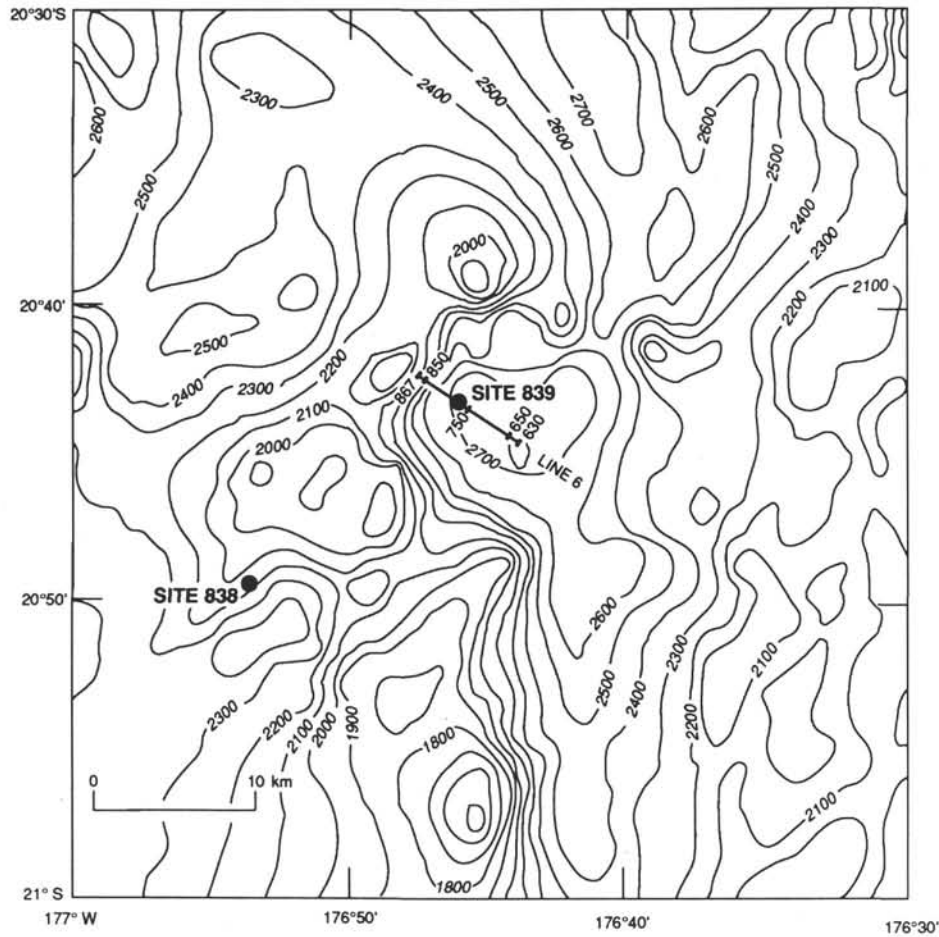


Figure 2. Detailed bathymetry showing Sites 838 and 839 and location of seismic line 6 across Site 839 with shotpoints annotated. Contours in meters; contour interval = 100 m.

in which the site was located. A basal sedimentary unit overlying and onlapping basement dips westward, and an angular unconformity in the middle of the sedimentary section separates these dipping beds from an upper, near-horizontal, westerly onlapping sedimentary unit. Total sediment thickness overlying basalt is 214.15 m. Sediments are predominantly nanofossil ooze in upper Unit I (middle Pleistocene, 17.85 m thick), and interbedded volcanoclastic turbiditic sands, silts, and gravels and nanofossil ooze in Units II (late Pliocene, 81.65 m thick) and III (late Pliocene; 114 m thick). The permeabilities of these sediments are reported by Lavoie et al. (this volume).

Site 839 penetrated igneous rocks from 205.85 to 218.2 mbsf in Hole 839A and from 214.15 to 497.26 m in Hole 839B, with one interbedded sedimentary unit (256.81–266.40 mbsf). The igneous rocks were divided into four major (>10 m thick) igneous units (Units 1, 3, 4, and 9; Table 1) and four minor (<10 m thick) igneous units (Units 2, 5, 6, 7, and 8; Table 1). All the basalts are very to extremely fresh with either little or minor alteration.

The sampled basalts are characteristically vesicular, and many of the units are comprised of mainly thin bedded flows or pillows (Table 1). The vesicularity could create a high internal permeability, and the large number of flow units could allow for large amounts of void space between flows or around pillows and, hence, a high interflow permeability. The high average porosity of most of the units, 32%–50% (Table 1) as determined from the compensated neutron porosity logging tool, indicates that for most of the basalts, 15%–35% of the porosity could be found in fractures or voids.

The packer was set at two depths (398.2 and 326.9 mbsf) within the basalts in Hole 839B. Permeability was measured only at the first set. The set at 398.2 mbsf sampled the permeability of Unit 9 (362.93–

497.26 mbsf), a thin- to medium-bedded basalt (2–4 glassy or fine-grained flow margins per meter) with 10%–20% vesicles (Table 1).

PACKER EXPERIMENT: EQUIPMENT AND PROCEDURES

Equipment

Permeability in Hole 839B was measured using a resettable, single drill-string packer manufactured by TAM International of Houston, TX; the operation of this packer on board the *JOIDES Resolution* is described by Becker (1990a, 1990b, 1991), from which much of the following discussion is taken. The packer uses a 1.2-m-long inflatable rubber element to isolate a section of the borehole. For Leg 135, the packer was configured as a single-packer, meaning that only one inflatable element was used in the borehole, and that the section isolated lies between the packer and the bottom of the borehole. The packer was seated twice in Hole 839B (at 398.2 and 326.9 mbsf).

Once the packer is lowered down the borehole, inflation of the packer element is enabled by a free-falling, retrievable “go-devil,” which keys into the packer inflation subassembly, where a rubber seal on the go-devil directs seawater pumped from the ship into the inflatable packer element. When the go-devil is seated in the packer control assembly, rig pumps can be used to pressurize the packer element to (in this experiment) 10.34 MPa, which will inflate the packer element. When the packer element is fully inflated, gripping the borehole wall, and holding the bottom-hole assembly in the hole, then the drill-string heave compensator is adjusted to transfer and maintain a weight of 6800–8165 kg downward onto the packer; the weight is provided with drill collars located just above the packer. This weight, in turn, shifts

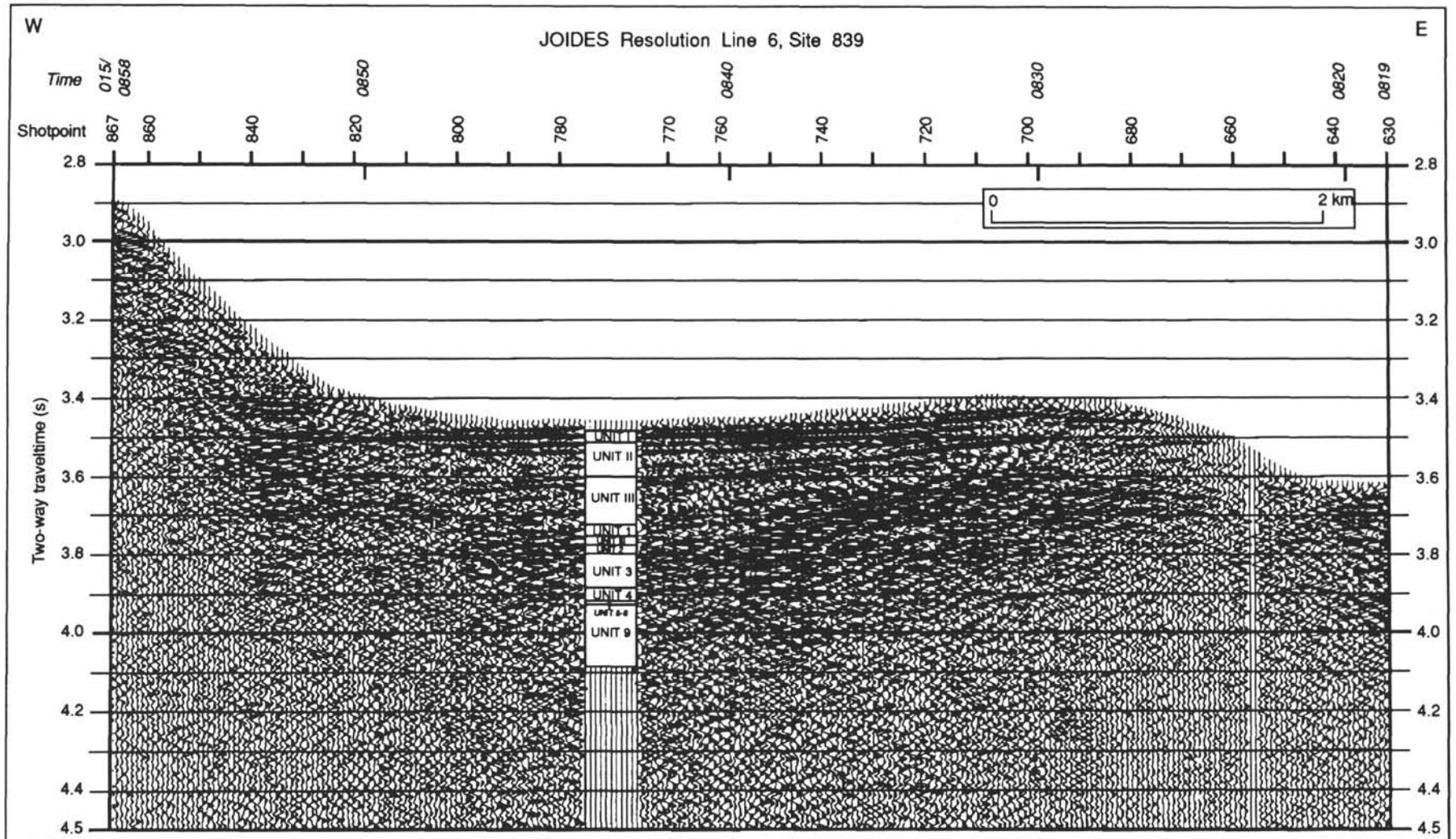


Figure 3. Part of migrated seismic line 6 over Site 839 showing flanking ridge and basin and fault that uplifts the sediment pond containing Site 839. The lithologic column is spliced into the line at the location of Hole 839B. Location of seismic line shown in Figure 2.

Table 1. Summary of basalt unit thickness, vesicularity, number of flow units, and average porosity, Site 839.

Basalt unit	Depth (mbsf)	Thickness (m)	Vesicularity (%)	Flow units (contacts/m)	Average porosity (%)	Possible fracture or void porosity (%)
1	214.15–256.81	42.66	25–30	0–1	32	2–7
2	266.40–276.06	9.66	10–15	2	45	30–35
3	276.06–334.33	58.27	20–30	3–8	49	19–29
4	334.33–353.30	18.97	30	5	51	21
5	353.30–353.43	0.13	8–10	—	—	—
6	353.43–353.54	0.11	15–20	—	—	—
7	353.54–362.90	9.36	10–15	—	48	33–38
8	362.90–362.93	0.03	15–20	—	—	—
9	362.93–497.26	134.33	10–20	2–4	43	23–33

Notes: Average porosity is determined by averaging the porosity measured by the neutron porosity logging tool over the basalt unit interval. Unit depths, vesicularity, and number of contacts/m are from Parson, Hawkins, Allan, et al. (1992), "Site 839" chapter. The average fracture/void porosity is estimated from the average porosity minus the vesicular porosity. Fractures and void spaces could give the basalts a high permeability.

a control tube in the packer to close off inflate/deflate ports and lock the packer element in the inflated position. When the element is locked off, the interval below the packer is open to fluid pressure applied by the shipboard pumps. A packer set can be considered mechanically successful if the inflated packer holds inflation pressure for 5–10 min before the packer is locked in the inflated position, and if the inflated packer is able to hold the weight applied on the packer by the drill string. A successful packer inflation does not, however, guarantee a hydraulic seal by the packer. After completion of testing, the packer is deflated by pulling up on the drill string at the rig floor, opening the inflate/deflate port, and allowing the packer element to deflate. About 1/2 hr is allowed for the packer to depressurize and deflate before it is moved.

The go-devil also carries pressure recorders (in this case, two calibrated mechanical Kuster K-3 recorders) to monitor downhole fluid pressures in the isolated, pressurized zone during the experiment. The gauges were retrieved at the end of the inflate/deflate cycle of the packer at each inflation depth. The Kuster pressure charts were converted to time and pressure readings after the experiment, and these readings along with the fluid flow rate measurements form the primary data needed to calculate a permeability. About 200–400 time/pressure points were read from the original 5- × 10-cm analog record using a microscopic caliper with a resolution of one part in 10,000 or about 0.004 MPa on the pressure axis.

The entire drill string, as well as the isolated zone in the borehole, is pressurized during testing. A pressure transducer in the high pressure line leading into the borehole is monitored at the driller's operating station to provide a real-time indication of downhole events.

Pressure Tests

Two kinds of pressure tests were run in Hole 839B. The first kind were pulse tests, which require rapid pumping of fluid into the shut-in borehole and drill string, and monitoring the decay rate of the pressure buildup from the pulse. The procedure is designed to approximate an instantaneous increase in pressure in the borehole. If the rate of decay is sufficiently slow (perhaps 30 min or more), then the permeability can be determined from the resulting record of pressure decay vs. time. If the decay rate after a pulse test is rapid (< about 15 min), then the pulse test will give inaccurate results, and the second kind of pressure test, an injection test, is run. On Leg 135, pulse tests were run by pumping water into the shut-in borehole until pressures measured on board were either 3.45 or 6.89 MPa. The amount of water injected into the borehole was measured by counting the number of strokes of the mud pump during the injection phase. Each stroke pumps a volume of 18.9 L, with a stroke per minute equivalent to about 0.315 L/s.

During an injection test, water is pumped into the shut-in hole at a constant rate for a period of time (in our case, from 20 min to 1 hr),

and the build up of pressure in the hole allows a calculation of permeability (see Becker, 1990a, 1990b, 1991). At Hole 839B, injection tests were run from 35 to 100 strokes/min (11.04–31.55 L/s). During these tests, the rate of injection was kept constant within about 5%. The actual rates were determined by counting the strokes of the mud pump.

Calculation Procedures

The calculation procedures for determining permeability for both slowly decaying pulse test and slowly increasing pressures during injection tests are given in detail by Becker (1990a). At Hole 839B, pulse tests decayed too rapidly for the pulse test calculation to be used. However, the first injection test at 398.2 mbsf showed a slowly increasing pressure rise during the course of the test, and a permeability can be calculated via the methods described by Becker (1990a).

In this case, the rise of pressure in the borehole as injection proceeds for a fairly long time is analogous to the rise of temperature of a heated needle probe used to measure thermal conductivity of sediments, and is described by nearly the same equation (see Becker, 1990a, 1991, for discussions):

$$P(D,t) = (q\mu/4\pi kL)\ln(\gamma\phi\mu C_i D^2/4\kappa t),$$

where q is the injection rate or quantity of water pumped per unit time (m^3/s) and is assumed to originate as a line source at the borehole; k is the permeability (m^2); L is the length of hole below the packer (m); D is the average hole diameter (m); t is time; γ is Euler's constant; ϕ is porosity; μ is the dynamic fluid viscosity; and C_i is the compressibility of the fluid in the isolated zone. From this, the transmissivity and average permeability of the isolated zone can be determined directly from the slope of a plot of pressure vs. the natural log of time, given a measured constant injection rate (Becker, 1990a).

An alternate method of calculating permeability was also used for the injection tests at 398.2 mbsf. During both tests, a relatively steady pressure response was obtained at the end of the first injection test and throughout the second injection test. For a constant-rate injection test where a steady pressure response is observed, Glover's formula (Anderson and Zoback, 1982; Zoback and Anderson, 1983) gives formation or bulk permeability:

$$k = cq \ln(2LD)/2\pi LH,$$

where $c = \mu/g\rho$ when μ is the fluid viscosity (Pa-s), g is the acceleration caused by gravity (m/s^2), and ρ is the fluid density (kg/m^3); H is the net head acting on the formation, given by $H = P/\rho g$, where P is the overpressure measured in the borehole below the packer and ρ , g , k , q , L , and D are as defined above. Thus,

$$k = \mu q \ln(2LD)/2\pi LP.$$

Following Anderson et al. (1985a) and Becker (1990a), we use Gartling's (1977) equation $\mu(10^{-3} \text{ Pa}\cdot\text{s}) = 16.68T^{-0.8987}$, with T in $^{\circ}\text{C}$ to determine the temperature-dependent viscosity of seawater. At a temperature of 4°C for the injected water (we assume that the injected water is cooled to the bottom temperature measured at Site 839), the resulting fluid viscosity of seawater is $\mu = 0.0048 \text{ Pa}\cdot\text{s}$. The average hole diameter, $D = 0.352 \text{ m}$, was calculated by averaging the caliper measurements obtained during logging of the hole. The length of the borehole isolated below the packer is uncertain and will be discussed later. All calculations assume axis symmetric flow away from the borehole and require that the packer make a hydraulic seal with the borehole wall.

OPERATIONS

Operations Summary

During logging operations, we picked possible sites for the packer experiment based on hole characteristics observed on the caliper logs. These locations were selected because the borehole walls were smooth with no breakouts, the width was sufficiently narrow for the packer to close off the borehole successfully, and the smooth section was long enough to give a good target for final positioning of the packer element. Velocity and density logs were used to give an indication of the competency of the section at these locations, and final site selections were made from this examination and from the Formation MicroScanner (FMS) caliper log. Based on these logs, two sites were selected at 398.2 and 326.9 mbsf. At the deepest site, the target section was 8.5 m long, with a borehole diameter between 0.28 and 0.33 m. The second site was 7.3 m long, with a borehole diameter from 0.33 to 0.38 m. At both sites, the hole was moderately elliptical, but we did not consider this to be a serious problem in sealing the hole with the packer element.

At both 398.2 and 326.9 mbsf, the packer was set and inflated successfully. In each case, the packer inflation pressure of 10.34 MPa held for about 10 min, with 6800 kg of weight set down on the packer with the drill string at the 398.2 mbsf set, and with the weight raised to 8165 kg at the 326.9 mbsf set. In both cases, all signs on board indicated that the packer element was successfully gripping the borehole wall.

At the first set at 398.2 mbsf, two pulse tests were run, at 3.45 and 6.89 MPa, as measured with the on-board pressure transducer. In both cases, pressures recorded on the on-board readout decayed rapidly, indicating an immediate pressure drop-off in the shut-in section of the borehole and drill string. The rapid decay indicated either a high permeability or a packer leak. Two injection tests were run to test the possibility that the basalt surrounding the borehole was extremely permeable (Table 2). In both injection tests, the pressure rise at the beginning of the test and falloff at the end were extremely rapid, and a flat pressure response during the injection phase was observed on the on-board pressure readout. After the second injection test, the packer was deflated and unseated, and the Kuster recorders were recovered, reset, and sent back down the hole with the go-devil.

With the packer reset at 326.9 mbsf, two pulse tests of 3.45 and 6.89 MPa were run; both decayed rapidly after pumping ceased, indicating

as before either a high permeability or a packer leak. Four injection tests were run (Table 2; for operational details, see Parson, Hawkins, Allan, et al., 1992, pp. 407–410 and 455–462). Again, all four tests yielded rapid pressure rises, flat on-board pressure responses during injection, and an immediate pressure drop when fluid injection ceased. After the fourth test the packer was unseated, deflated, and retrieved. Overpulls of 23,000 and 18,000 kg were required to pull the packer from the hole, indicating that the packer element was stuck within the hole and was probably not entirely deflated.

When the packer was recovered at the rig floor, the packer rubber element was pulled inside out, and several steel cables within the element were broken. However, the surface of the recovered element was only slightly worn and abraded. Some striations and pockmarking caused by pressure from the hole wall were evident; basically, however, the packer was in excellent condition, except for the tear caused by extraction of the packer from the hole.

Kuster Pressure Recorder Results and Implications

Kuster pressure charts for both packer sets show only small increases in pressure in the borehole below the packer. A problem for both sets is that Kuster Gauge 860909 read about 0.4 MPa higher than Gauge N9542, and the recorded hydrostatic pressure was also about 0.4 MPa higher than the pressure calculated for the water depth to the packer. Therefore, to correct this static instrument calibration error, the pressure vs. time curve for Gauge 860909 was shifted down by 0.4 MPa to match the curve for Gauge N9542.

The Kuster pressure chart for the first packer set confirmed the observations made during the test that pressure decayed to 0 MPa almost immediately after each pulse and injection test (Fig. 4). The pressure increase over the hydrostatic baseline pressure during the first injection test was 0.228 MPa on Kuster Gauge N9542 and 0.345 MPa on Kuster Gauge 860909. A pressure rise during the first injection test was observed on the Kuster pressure data with the pressure attaining a relatively constant value by the end of the test. We calculated a permeability for this test based both on the pressure rise vs. time and on the constant pressure (Glover's formula) techniques.

During the second injection test, the pressure increase was 0.448 and 0.490 MPa for Gauges N9542 and 860909, respectively. On the second test, the Kuster-recorded pressure rose immediately to a relatively constant level and then decayed slightly, rather than increasing during the course of the test. Because the amount of pressure decay is small, we still calculated a permeability for the second test, assuming that an average of the measured pressures is a valid approximation to the steady-state pressure response of Glover's formula.

For the second set (Fig. 5), pressures shown during the injection tests for both Kuster pressure charts were very small and highly irregular. For Kuster Gauge 860909, only the second injection test yielded a quasi-steady state pressure that might be a valid measure of the permeability. The third and fourth tests yielded a rising and falling pressure response, with no steady-state behavior. For Kuster Gauge N9542, no pressure response was observed on the second injection test, injection test three yielded an increasing pressure, and test four yielded a decreasing pressure.

Mechanical problems with the packer occurred during the second set (Parson, Hawkins, Allan, et al., 1992, pp. 407–410). Injection tests at high injection rates yielded only small pressure increases at the Kuster gauges. For example, the fourth and longest injection test created peak pressure increases of 0.097 MPa on Kuster Gauge N9542, which decayed to about 0.052 MPa during the course of the test, yet the on-board pumping pressure of 20.34 MPa approached the limits of the pumping equipment. Calculated frictional pressure drops through the pumps, connecting hoses, and drill pipe are about 15% of the total measured on-board pressure, leaving a residual pressure that should have been seen as a significant pressure increase in the shut-in section of the borehole.

Table 2. Summary table of injection tests run at Hole 839B.

Packer depth (mbsf)	Injection test	Duration (min)	Strokes per minute	Fluid injection rate (L/s)
398.2	1	41	50	15.78
	2	33	100	31.56
326.9	1	6	50	15.78
	2	21	35	11.04
	3	32	45	14.20
	4	62	59	18.61

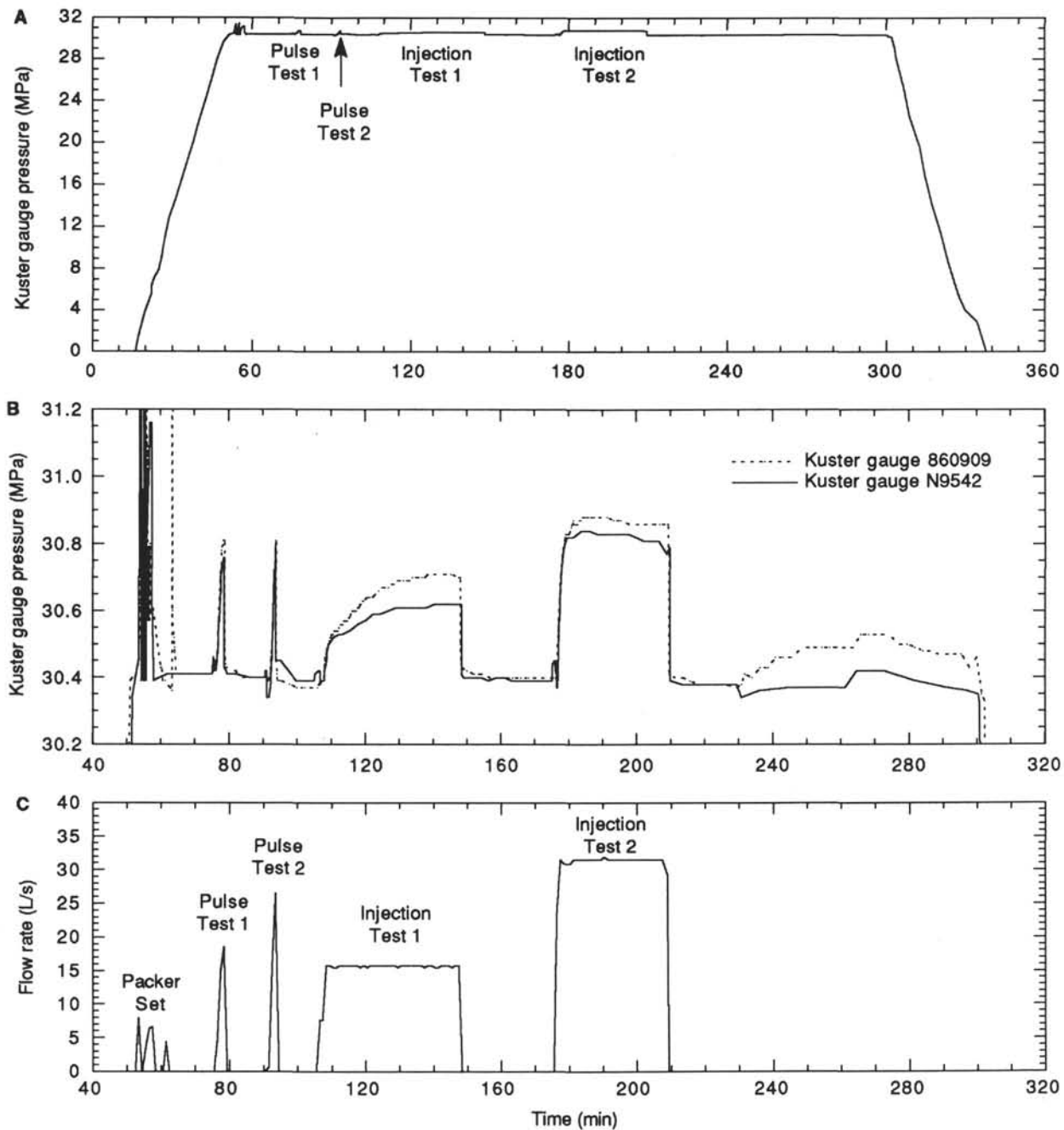


Figure 4. Kuster charts for first packer set at 398.2 mbsf. Kuster pressure charts are shown full scale and enlarged to reveal pressure changes during pulse and injection tests; the injection rate is shown beneath the enlarged Kuster chart. Kuster 860909 is shifted downward by -0.4 MPa to match the baseline of Kuster N9542. **A.** Complete Kuster pressure chart. **B.** Detail of injections. **C.** Fluid injection rates based on digital data recorded continuously during the experiment.

On recovery of the go-devil after the second packer set, a seal separation ring on the go-devil was found to have rotated 45° with respect to the mandrel flow holes, through which water flows to inflate the packer element and, after the packer is set, to reach the isolated borehole. With the ring rotated, pressure would be required to pump water through the plugged go-devil mandrel flow holes. As these flow holes are also used in deflating the packer element, their partial blockage could lead to only partial deflation of the packer element, resulting in the damage to the element that occurred when the packer was pulled from the hole.

At the end of Leg 135, tests were done to experimentally measure pressure losses for this possible mechanical malfunction. The pressure rise obtained when the seal separation ring on the go-devil closed off the mandrel flow holes was 20.37 MPa at 50 strokes/min, very similar to what was observed during the second packer set (20.3–20.4 MPa). As the seal separation ring was in the rotated position when the packer was recovered, we conclude that this was the cause of the high pressures observed during the packer experiment.

Because of the highly irregular and extremely small pressure responses during the second packer set, and because of the demonstrated

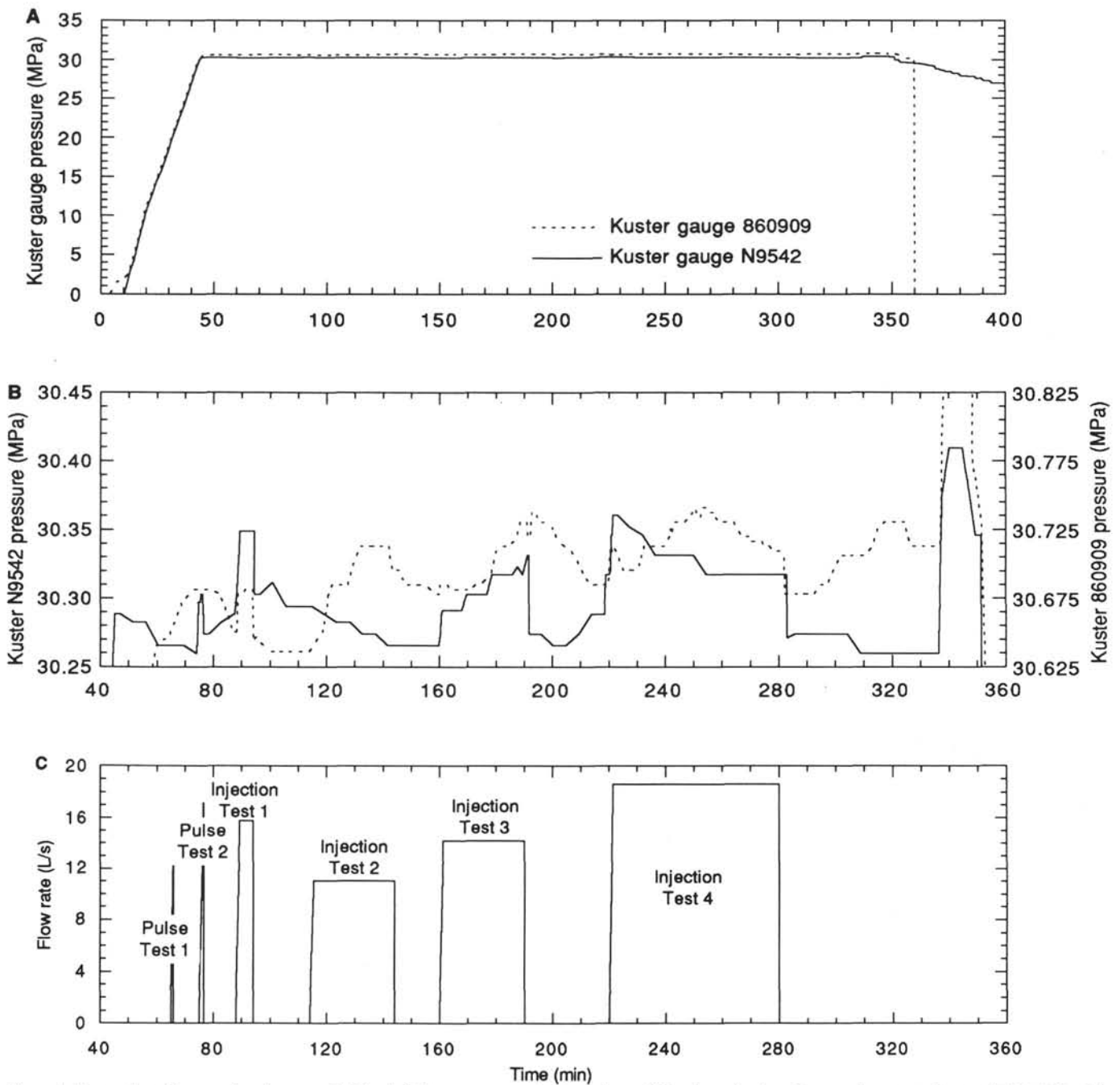


Figure 5. Kuster charts for second packer set at 326.9 mbsf. Kuster pressure charts are shown full scale and enlarged to reveal pressure changes during pulse and injection tests, injection rates are shown beneath the enlarged Kuster chart. Kuster Gauge 860909 is shifted downward by -0.4 MPa to match the baseline of Kuster Gauge N9542. **A.** Complete Kuster pressure chart. **B.** Detail of injections. **C.** Fluid injection rates, constructed from average pump rates recorded during the experiment.

mechanical problems, we concluded that the resulting data are unreliable and invalid. No permeabilities were calculated for the second set.

PERMEABILITY CALCULATION

For the permeability calculations, we used the Kuster measured borehole pressures, the fluid injection rate measured on the ship, and the average borehole diameter determined from the log calipers. The length of borehole tested is somewhat variable. The borehole length below the first packer set was about 119 m (total depth [TD] of 517.2 mbsf; packer depth of 398.2 mbsf). However, the last logging run with the FMS tool found bottom at 465.9 mbsf, 51.3 m above the drilled

TD. In this case, the total borehole exposed below the packer could be as little as 67.7 m. More likely, some part or all of the borehole below the blockage remained open to the fluid pumped into the hole. Thus, the minimum and maximum lengths of the borehole give a range of possible permeabilities.

Permeabilities were calculated for the first injection test at 398.2 mbsf based on the slope of the best-fit line to the plot of pressure difference vs. natural log of time (Fig. 6). These values are shown in Table 3; they range from 0.6 to 1.6×10^{-12} m². The permeabilities calculated by Glover's formula for the two injection tests at 398.2 mbsf are shown in Table 4; they range from 1.9 to 4.7×10^{-12} m², consistent with, although somewhat higher than, the values shown in

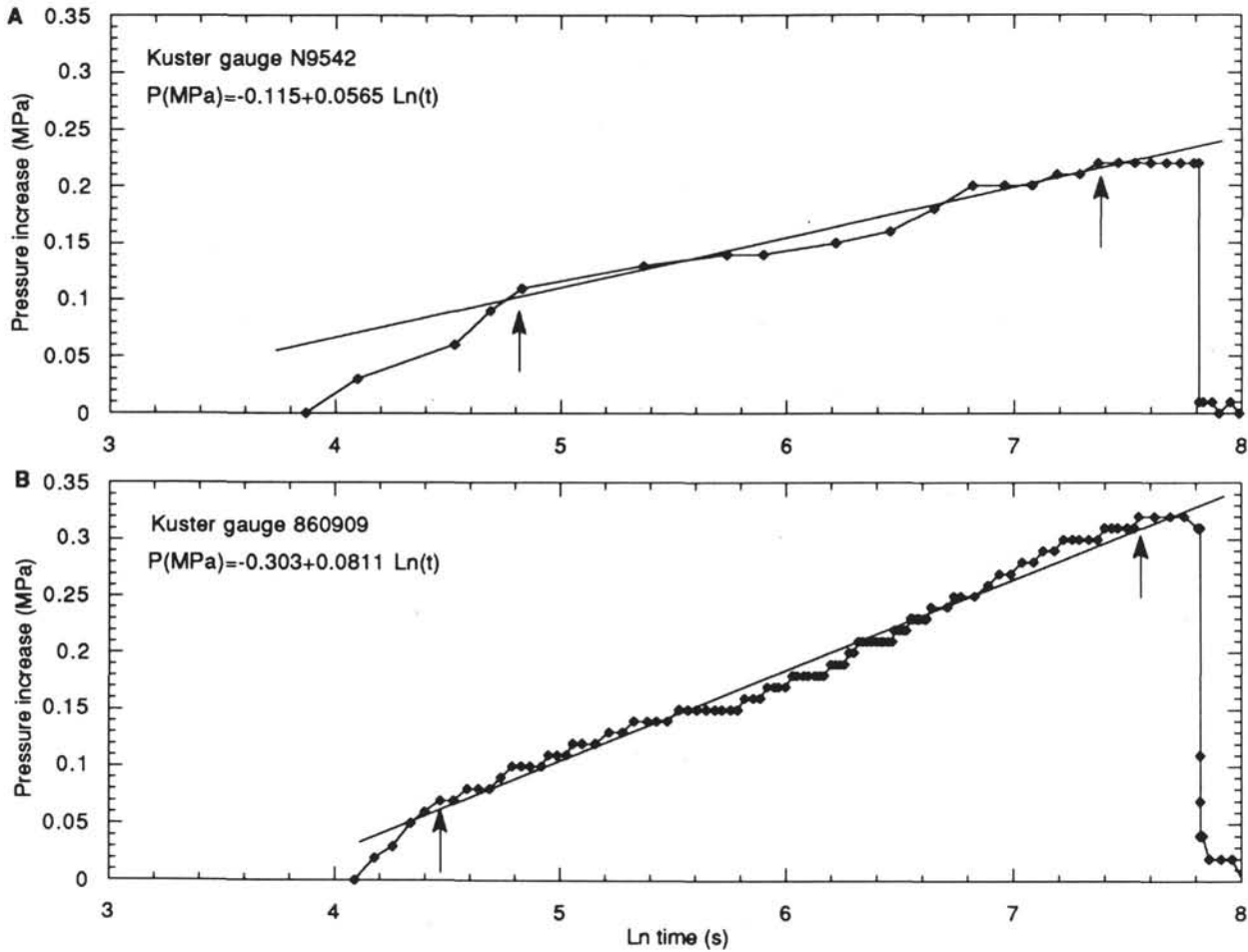


Figure 6. Plot of pressure increase (MPa) vs. Ln time (s) for the first injection test at 398.2 mbsf. The equation describes the line shown, which was obtained by a linear regression through the linear segment of the plot, chosen as the points lying between the arrows. Bulk permeability is calculated from the slope of this line. A. Plot for Kuster Gauge N9542. B. Plot for Kuster Gauge 860909.

Table 3. For all calculations, the range of values is about 1 to 5×10^{-12} m². The most probable value, based on the assumption that most or all of the borehole was open to injected fluid below the blockage at 465.9 mbsf, is about 1 to 3×10^{-12} m².

DISCUSSION

Comparison with Other DSDP and ODP Permeability Measurements

The permeability of pillow lavas and flows, similar to those measured in the Lau Basin, has been measured or estimated at Holes 395A (Mid-Atlantic Ridge) and 504B (Costa Rica Rift). At Hole 395A, Becker (1990b) reported a range from 10^{-12} to 10^{-14} m² for the permeability of basalt flows and pillows, although this permeability was estimated, not measured, from temperature logs. Packer measurements in basalt breccias, pillow lavas, and dolorites between 583 and 664 mbsf yielded a permeability of 10^{-17} to 10^{-18} m² (Hickman et al., 1984).

At Hole 504B, where the most extensive packer testing has occurred, the upper 200 m of basement, comprised of pillow lavas, had a permeability of 10^{-13} to 10^{-14} m² (Anderson and Zoback, 1982; Zoback and Anderson, 1983; Anderson et al., 1985a, 1985b; Becker, Langseth, and Von Herzen, 1983; Becker, Langseth, Von Herzen, and Anderson, 1983). Underlying sheeted dikes had a permeability of 10^{-17} to 10^{-18} m² (Anderson et al., 1985b; Becker, 1989).

At Hole 735B (near the Atlantis II Fracture Zone on the Southwest Indian Ridge), olivine gabbro had a permeability of 2.4×10^{-14} m²

Table 3. Permeabilities calculated for first set, first injection test using slope of best-fit line to a plot of pressure difference vs. natural log of time.

Kuster gauge	Borehole length (m)	Permeability $\times 10^{-12}$ (m ²)
N9542	67.7	1.58
860909	67.7	1.10
N9542	119.0	0.90
860909	119.0	0.63

Table 4. Permeability calculations using Glover's Formula for Hole 839B injection tests.

Packer depth (mbsf)	Injection test	Kuster gauge	Borehole length (m)	Pressure increase (MPa)	Fluid injection rate (L/s)	Permeability $\times 10^{-12}$ (m ²)
398.2	1	N9542	67.7	0.227	15.78	4.66
		860909	67.7	0.344	15.78	3.07
	2	N9542	119.0	0.227	15.78	2.90
		860909	119.0	0.344	15.78	1.92
398.2	2	N9542	67.7	0.448	31.56	4.73
		860909	67.7	0.490	31.56	4.33
	2	N9542	119.0	0.448	31.56	2.95
		860909	119.0	0.490	31.56	2.70

(Becker, 1991). Goldberg et al. (1991) note that the in-situ permeability strongly correlated with and was controlled by fracturing.

Thus, measurements obtained from the pillow basalts and thin-bedded flow units of Hole 839B yielded a higher permeability than measured at other sites, although the measured permeability is at the upper range of permeability estimated for pillow lavas of Hole 395A.

As a further comparison, Lavoie et al. (this volume) measured hydraulic conductivities and consolidation characteristics on samples from the Lau Basin sites. Samples were measured in a controlled laboratory triaxial apparatus, with hydraulic conductivity measured after primary consolidation was complete. Hydraulic conductivity can be converted to permeability by the relation $K = (\rho g/\mu)k$, where K is hydraulic conductivity (m/s), ρ is fluid density (kg/m^3), g is gravity (m/s^2), μ is the fluid viscosity, and k is permeability (m^2). The highest measured value was from vitric sands recovered from Hole 839A; these sands had a permeability of about $1.4 \times 10^{-13} \text{ m}^2$, assuming fluid viscosity for water at 20°C (similar to temperatures measured in the borehole during logging). Permeabilities in nannofossil oozes ranged from about 5 to $10 \times 10^{-16} \text{ m}^2$. The least permeable sediments were clayey sediments, with a permeability of about $4 \times 10^{-17} \text{ m}^2$. Because these sediments are relatively unconsolidated, fractures and void spaces should be minimal, and these measurements may be close to the formation permeability. Thus, the packer-measured bulk permeability of the upper crustal pillow basalts is greater than the permeability of the overlying sediments.

Validity of Calculated Permeabilities

Are the calculated permeabilities valid? The measurement of a permeability with a packer has an inherent ambiguity: we cannot prove that the packer did not leak, as the borehole above the packer is open to the ocean. A criteria for a packer seal is that the pressure data show steadily decreasing pressure on pulse tests, or gradually increasing pressure on injection tests, with a gradually decreasing pressure after injection ceases (Becker, 1990a, 1990b, 1991). The first injection test at 398.2 mbsf partially met these criteria, but generally the system was not well behaved in the required fashion, with virtually instantaneous pressure rises and drops, and, in the second injection test, with slightly decreasing pressure during the course of the test. Thus, despite the fact that all the on-board criteria for a successful packer set were met (i.e., a high inflation pressure held for about 10 min, and the set packer held the required weight), we have no assurance that the packer sealed the borehole. Thus, the measured values must be considered as an upper bound, and real formation permeabilities may be lower.

The permeability determined from the packer experiment may not be surprising, given that basalts sampled in the hole have from 30% to 50% average porosity based on the results obtained with the neutron porosity logging tool (Table 1 and Fig. 7), and the basalts are almost all highly vesicular and many are thin bedded. These factors could translate to both a high permeability within the basalt and a high void or fracture permeability between basalt flows or pillows. The vesicularity will presumably be included within the porosity measured during geophysical logging, so that the difference between the porosity and the vesicle pore space may give an estimate of fracture and interflow/pillow void porosity. Each of these factors is estimated in Table 1.

The neutron porosity logging tool may overestimate the porosity within basalts. The tool measures porosity based on absorption of emitted neutrons by hydrogen nuclei in the formation, with the hydrogen assumed to be dominantly contained in water molecules. However, bound water contained within the formation can lead to overestimates of the porosity. This bound water is mainly associated with clays and other alteration minerals. Goldberg et al. (1991) make corrections to the neutron porosity log obtained in basalts and gabbros from Hole 735B. The correction is based on an alteration estimate derived from core samples and from the hydrogen yield log recorded with the in-

duced gamma-ray spectrometry tool. They note that even in areas of high alteration, the neutron porosity correction is only about 10%.

Basalts from Hole 839B are slightly to moderately altered, but below Unit 1 are mainly remarkably fresh and appear unaffected by any high temperature fluid alteration (Parson, Hawkins, Allan, et al., 1992, pp. 397–487). Thus, we conclude that the porosities measured with the neutron porosity tool and given in Table 1 are at most 10% higher than the actual porosity. Since alteration in the sampled basalts is mainly slight, the log porosity is mostly high by much less than 10%.

The packer at 398.2 mbsf measured the permeability of Unit 9. Unit 9 (362.93–497.26 mbsf) contained numerous glassy or fine-grained flow margins (2 to 4 contacts/meter), indicating a series of thin- to medium-bedded flows or pillows. The rocks of Unit 9 are conspicuously vesicular, with vesicle concentrations estimated between 10% and 20%, but extending as high as 35%. The average log porosity in the unit was 43%. Thus, as much as 30% of the measured porosity may be caused by voids and fractures.

Well logs (Fig. 7) give a further indication of the amount of void space in the basalts. Unit 1 is characterized by few contacts per meter (Table 1). The unit has a high density (about 2.6 g/cm^3), low porosity (average 32%), and high resistivity (Table 1 and Fig. 7). In contrast, units 2 through 8 all are mainly thin bedded, have a high percentage of possible fracture or void porosity (Table 1), and are characterized by a medium density (average about 2.2 g/cm^3), high porosity (45%–51%), and low resistivity.

Unit 9 is variable. The segment of Unit 9 between about 397 and 420 mbsf is similar in character to Units 2–8, with low density and low resistivity, and may therefore be thin bedded. The sections between 363 and about 397 mbsf, and below 430 mbsf have characteristics similar to the massively bedded Unit 1 with high resistivity and high density; however, they have a greater number of contacts per meter and are probably medium bedded. The packer was set at the top of the interval that appears to be thin bedded.

In summary, the basalt below the packer is at least in part composed of thin flows or pillow basalts that appear to have a high amount of void space around the pillows and between the flows, and hence could have a high formation permeability. The medium-bedded upper and lower parts of Unit 9 may be less permeable than the rest of the unit. However, because the formation permeability is controlled by the most permeable sections of the formation, the high void/fracture space in thin-bedded basalt should give a high formation permeability.

The region drilled at Site 839 may also be affected by faulting, as it lies on a tilted basement block. If the basalts are faulted, fracture permeability could also be significant. Our feeling is that the calculated permeabilities are not unreasonable when compared with the range of measurements taken elsewhere in similar rocks, and considering the physical nature of the rocks tested. Nevertheless, the calculated permeability is an upper bound; if the packer leaked, then the basalt formations could have a permeability lower than we measured.

Fluid Circulation in the Lau Basin

Several lines of evidence indicate high rates of fluid flow at Site 839 and in the Lau Basin in general. First, the temperature gradients and calculated heat-flow values are considerably lower than expected when compared with the theoretical heat-flow values of 175–200 mW/m^2 predicted for young oceanic crust (Anderson et al., 1977; Parsons and Sclater, 1977). During drilling operations, temperature measurements were made by pushing a temperature probe into unconsolidated and semiconsolidated sediments ahead of the drill bit. Because the probe is used in undrilled and thus undisturbed sediments, the measured temperatures should be immune from the effects of drilling fluid circulation. The temperature measurements determine vertical temperature gradients in the sediments and are combined with the measured thermal conductivity to determine heat flow (Parson, Hawkins, Allan, et al., 1992, p. 454). Thermal gradients range from

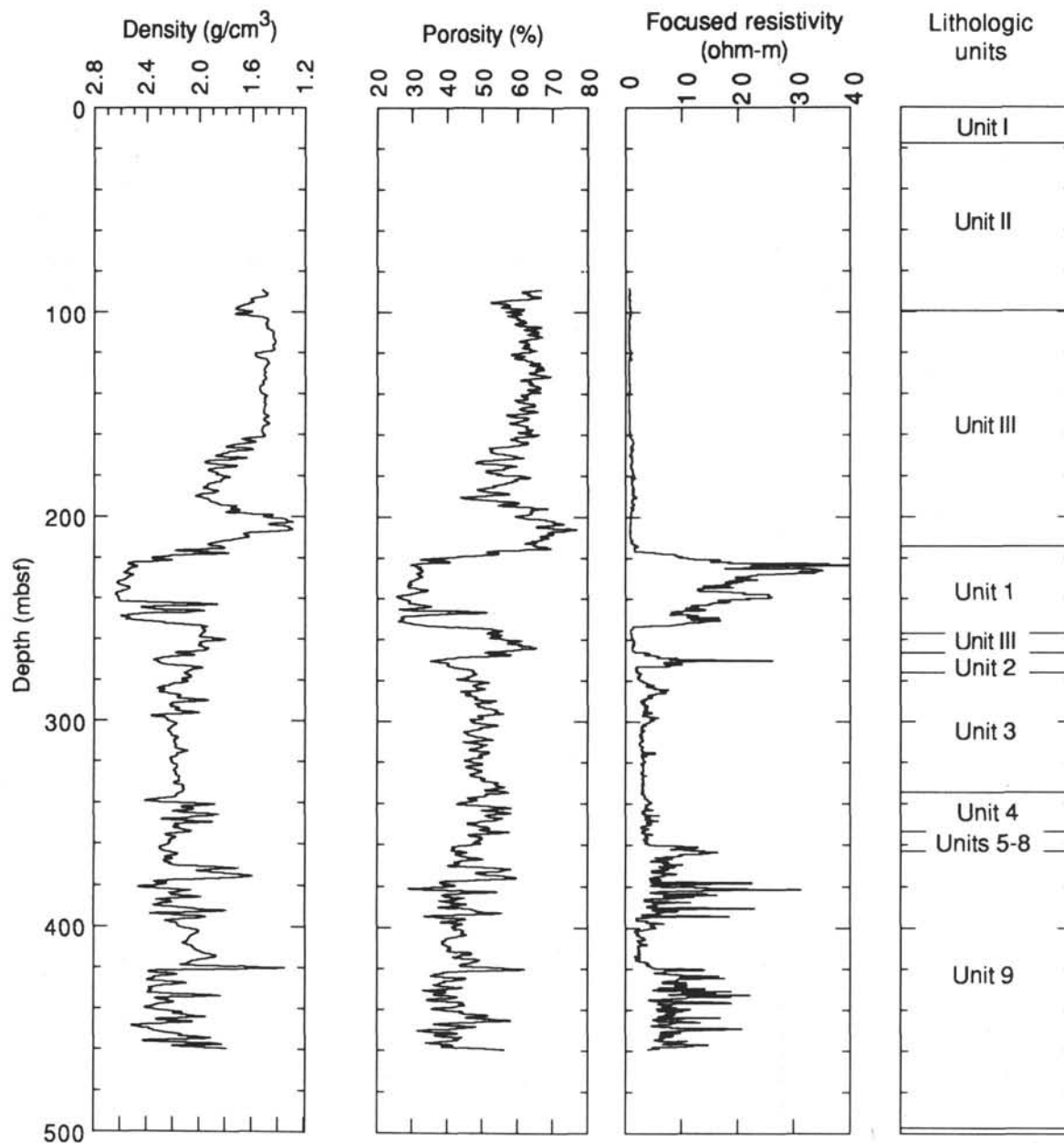


Figure 7. Geophysical well logs (density, porosity, and focused resistivity) and simplified lithologic column for Hole 839B. Density values have been plotted from high to low to better show correlation with porosity and resistivity values. The logs and lithologic chart were derived from Parson, Hawkins, Allan, et al. (1992, pp. 397–487).

a low of $0.7^{\circ}\text{C}/100\text{ m}$ at Site 839 to a high of $8.7^{\circ}\text{C}/100\text{ m}$ at Site 838, with heat-flow values of from $9.1\text{ mW}/\text{m}^2$ at Site 839 to $50.6\text{ mW}/\text{m}^2$ at Site 838 (Parson, Hawkins, Allan, et al., 1992). These low values indicate that fluid circulation in the backarc is sufficient to dissipate large amounts of heat.

The measured thermal gradients are not constant throughout the section. Measured values were slightly higher in the least permeable sediments, and were lowest in the most permeable vitric sandstones and gravels. The differences may be a result of high rates of fluid flow through the permeable sediments (Lavoie et al., this volume).

Additional evidence for fluid flow is that sediments in the basin are underconsolidated (Lavoie et al., this volume). Laboratory measurements show that these sediments can consolidate normally. Possible reasons for the underconsolidation include high sedimentation rates, or a high rate of upward or lateral fluid circulation through the system. Calculations of hydraulic conductivity indicate that the clayey nanno-

fossil oozes, the most impermeable of the sediments tested from the back arc sites, are still sufficiently permeable to allow passage of fluids through the sediments in periods of days or months if a sufficient driving force is available. Pressure and density differences caused by heat can provide such a driving force (Lavoie et al., this volume).

Finally, the chemistry of pore fluids extracted from the sediments and sedimentary rocks showed little variation throughout the sediment column and was similar to open seawater values, suggesting a circulation system open to exchange with seawater (Parson, Hawkins, Allan, et al., 1992, pp. 428–430).

The high permeability of the basalts measured during the packer experiment indicates that a high rate of fluid flow could be carried through the basalts. The well log data indicate that the most permeable sections are Units 2 through 8 and the segment of Unit 9 between 397 and 420 mbsf. If the massive bedding of Unit 1 and the thick-bedded upper and lower segments of Unit 9 have low fracture permeability,

then fluids could mainly be driven through the permeable zones between these units.

SUMMARY OF PERMEABILITY MEASUREMENTS AT HOLE 839B

A downhole packer was deployed in the basalts penetrated in Hole 839B, with the packer element inflated at 398.2 and 326.9 mbsf. Constant rate injection tests at the 398.2 mbsf yielded a permeability of 1 to 5×10^{-12} m² for the basalt formations below the packer. The measured permeabilities must be considered as an upper limit; if the packer leaked during the experiments, the basalt could be less permeable.

The basalts in Hole 839B are more permeable than basalts at other DSDP and ODP sites, where packer measurements yielded permeability values mainly from 10^{-13} to 10^{-14} m². However, the basalts measured at Site 839 are in part thin bedded. Based on well logs, these basalts have high porosity, only part of which can be a result of vesicularity within the basalts, with the remainder caused by a high amount of void and fracture porosity. Thus, the calculated permeability is not unreasonable for the known or inferred physical conditions of the drilled formations.

Temperature data, and the geochemical and geotechnical properties of the drilled sediments all indicate that the site is strongly affected by fluid flow. Much of this flow could be directed through highly porous and permeable zones within the basalts. The permeability measurements thus give an indication of where and how fluid flow may occur within the oceanic crust of the Lau Basin.

ACKNOWLEDGMENTS

The permeability measurements reported here would not have been possible without the expertise and hard work of P. Thompson and E. Pollard. We also gratefully acknowledge the SEDCO drill crew and drilling superintendent J. Tarbutton, especially for noticing and pointing out to us the rotated seal-separation ring after the second packer set, which allowed us to determine what the problems were. This report was improved by careful reviews by Homa Lee, Rob Kayen, Marcus Langseth, and Keir Becker. Errors in calibrations or calculations, and misunderstandings, if any are still present, are solely the responsibility of the authors. D. L. Lavoie's work was supported by NRL program element number 61153N.

REFERENCES*

- Anderson, R.N., Langseth, M.G., and Sclater, J.G., 1977. The mechanisms of heat transfer through the floor of the Indian Ocean. *J. Geophys. Res.*, 82:3391-3409.
- Anderson, R.N., and Zoback, M.D., 1982. Permeability, underpressures, and convection in the oceanic crust near the Costa Rica Rift, eastern equatorial Pacific. *J. Geophys. Res.*, 87:2860-2868.
- Anderson, R.N., Zoback, M.D., Hickman, S.H., and Newmark, R.L., 1985a. Permeability versus depth in the upper oceanic crust: in situ measurements

in DSDP Hole 504B, eastern equatorial Pacific. *J. Geophys. Res.*, 90:3659-3669.

- , 1985b. Permeability versus depth in the upper oceanic crust: in situ measurements in Deep Sea Drilling Project Hole 504B, eastern equatorial Pacific. In Anderson, R.N., Honnorez, J., et al., *Init. Repts. DSDP*, 83: Washington (U.S. Govt. Printing Office), 429-442.
- Becker, K., 1989. Measurements of the permeability of the sheeted dikes in Hole 504B, ODP Leg 111. In Becker, K., Sakai, H., et al., *Proc. ODP. Sci. Results*, 111: College Station, TX (Ocean Drilling Program), 317-325.
- , 1990a. A guide to formation testing using ODP drill-string packers. *ODP Tech. Note*, 14.
- , 1990b. Measurements of the permeability of the upper oceanic crust at Hole 395A, ODP Leg 109. In Detrick, R., Honnorez, J., Bryan, W.B., Juteau, T., et al., *Proc. ODP. Sci. Results*, 106/109: College Station, TX (Ocean Drilling Program), 213-222.
- , 1991. In-situ bulk permeability of oceanic gabbros in Hole 735B. In Von Herzen, R.P., Robinson, P.T., et al., *Proc. ODP. Sci. Results*, 118: College Station, TX (Ocean Drilling Program), 333-348.
- Becker, K., Langseth, M.G., and Von Herzen, R.P., 1983. Deep crustal geothermal measurements, Hole 504B, Deep Sea Drilling Project Legs 69 and 70. In Cann, J.R., Langseth, M.G., Honnorez, J., Von Herzen, R.P., White, S.M., et al., *Init. Repts. DSDP*, 69: Washington (U.S. Govt. Printing Office), 223-236.
- Becker, K., Langseth, M.G., Von Herzen, R.P., and Anderson, R.N., 1983. Deep crustal geothermal measurements, Hole 504B, Costa Rica Rift. *J. Geophys. Res.*, 88:3447-3457.
- Gartling, D.K., 1977. Convective heat transfer analysis by the finite element method. *Comput. Methods Appl. Mech. Eng.*, 12:365-382.
- Goldberg, D., Broglia, C., and Becker, K., 1991. Fracturing, alteration, and permeability: *in-situ* properties in Hole 735B, Atlantis II Fracture Zone, southwest Indian Ocean. In Von Herzen, R.P., Robinson, P.T., et al., *Proc. ODP. Sci. Results*, 118: College Station, TX (Ocean Drilling Program), 261-270.
- Hickman, S.H., Langseth, M.G., and Svitek, J.F., 1984. In situ permeability and pore-pressure measurements near the mid-Atlantic Ridge, Deep Sea Drilling Project Hole 395A. In Hyndman, R.D., Salisbury, M.H., et al., *Init. Repts. DSDP*, 78 (Pt. 2): Washington (U.S. Govt. Printing Office), 699-708.
- Parson, L., Hawkins, J., Allan, J., et al., 1992. *Proc. ODP, Init. Repts.*, 135: College Station, TX (Ocean Drilling Program).
- Parsons, B., and Sclater, J.G., 1977. An analysis of the variation of ocean floor bathymetry and heat flow with age. *J. Geophys. Res.*, 82:803-827.
- Zoback, M.D., and Anderson, R.N., 1983. Permeability, underpressures, and convection in the oceanic crust at Deep Sea Drilling Project Hole 504B. In Cann, J.R., Langseth, M.G., et al., *Init. Repts. DSDP*, 69: Washington (U.S. Govt. Printing Office), 245-254.

* Abbreviations for names of organizations and publication titles in ODP reference lists follow the style given in *Chemical Abstracts Service Source Index* (published by American Chemical Society).

Date of initial receipt: 30 June 1992

Date of acceptance: 30 June 1993

Ms 135SR-150